

The sources of streamwater to small mountainous rivers in Taiwan during typhoon and non-typhoon seasons

Tsung-Yu Lee¹  · Nien-Ming Hong² · Yu-Ting Shih³ · Jr-Chuan Huang³ · Shuh-Ji Kao⁴

Received: 30 December 2014 / Accepted: 10 August 2015 / Published online: 19 August 2015
© Springer-Verlag Berlin Heidelberg 2015

Abstract The dynamics and behaviors of streamwater chemistry are rarely documented for subtropical small mountainous rivers. A 1-year detailed time series of streamwater chemistry, using non-typhoon and typhoon samples, was monitored in two watersheds, with and without cultivation, in central Taiwan. Rainwater, soil leachate, and well water were supplemented to explain the streamwater chemistry. The concentrations of fluoride, chloride, sulfate, magnesium, potassium, calcium, strontium, silicon, and barium of all the water samples were measured. Principal component analysis and residual analysis were applied to examine the mechanisms of solute transport and investigate possible sources contributing to the streamwater chemistry. In addition to the influence of well water and soil leachate on streamwater chemistry during non-typhoon period, overland flow and surface erosion affect streamwater chemistry during the typhoon period. The latter has not been discussed in previous studies. Surface erosion is likely to be an end member and non-conservatively mixed with other end members, resulting in a previously unobserved blank zone in the mixing space. This has a particularly great impact on small mountainous watersheds, which suffer from

rapid erosion. Moreover, fertilizer contaminates agricultural soil, making soil water end members more identifiable. To our knowledge, this study is the first to clearly illustrate the dynamics and sources of streamwater chemistry of small mountainous rivers that are analogous to rivers in Oceania.

Keywords Hydrology · Taiwan · Typhoon · Mixing model · End member · Streamwater chemistry

Introduction

Catchment systems are hydrologically complex and have varied flow pathways, which contribute to the stream discharge under different hydrological conditions and control streamwater chemistry (Christophersen et al. 1990; Christophersen and Hooper 1992; Burns et al. 2001; Katsuyama et al. 2001; Chaves et al. 2008; Barthold et al. 2011). Mixing models of surface water chemistry is a useful method of examining how different sources and mechanisms control the export of nutrients and chemicals at the watershed scale, improving our understanding of ecosystem functionality (Tsai et al. 2009; Chang et al. 2013), chemical weathering (Anderson and Dietrich 2001; Anderson et al. 2002; Calmels et al. 2011), hydrological processes (Ali et al. 2010; Barthold et al. 2010; Inamdar et al. 2013), instream biological processes (Mulholland and Hill 1997), and even the structure of hydrological models (Hooper et al. 1990).

Hooper et al. (1990) first developed end member mixing analysis (EMMA), which is a common tool used to investigate and understand runoff sources and their contributions to streamwater based on the assumption of conservative mixing, when the necessary information on end members is available (Christophersen and Hooper 1992; Barthold et al. 2010). Hooper (2003) further developed diagnostic tools that include

Responsible editor: Philippe Garrigues

✉ Tsung-Yu Lee
tylee@ntnu.edu.tw

¹ Department of Geography, National Taiwan Normal University, Taipei, Taiwan

² Graduate Institute of Earth Science, Chinese Culture University, Taipei, Taiwan

³ Department of Geography, National Taiwan University, Taipei, Taiwan

⁴ State Key Laboratory of Marine Environmental Science, Xiamen University, Xiamen, China

two procedures: principal component analysis (PCA) followed by residual analysis, to determine the approximate rank of the dataset and to assess the lack of fit to the data. This permits identification of processes that violate the assumptions of the mixing model and can suggest the dominant processes controlling streamwater chemical variation without the explicit identification of end members. However, such applications have mostly been applied to small catchments (<100 ha), where the influence of landscape heterogeneity and catchment complexity is very small, in the temperate and tropical zone (Acuña and Dahm 2007; Fröhlich et al. 2008; Elsenbeer et al. 1995; Hooper 2003; James and Roulet 2006; Chaves et al. 2008; Katsuyama et al. 2009). Few studies have focused on small subtropical mountainous rivers, where river behaviors are characterized by episodic events and high water (Kao and Milliman 2008; Lee et al. 2013; Milliman and Farnsworth 2013).

Taiwan is a subtropical mountainous island with a maximum elevation of approximately 4000 m above sea level and 70 % of its area is above 100 m above sea level. Taiwan experiences three to five typhoons per year and the island-wide annual rainfall is approximately 2400 mm, which is over three times the global average (Legates 1995). Located at the collision boundary of the Philippine Sea Plate and the Eurasian Plate, Taiwan has uplift rates of 2–10 mm year⁻¹ (Liu and Yu 1990). Taiwan has the highest physical denudation rate and the highest chemical weathering rate in the world (You et al. 1988; Li et al. 1997; Dadson et al. 2003; Milliman and Farnsworth 2013). This is largely caused by the abundant rainfall (as a carrier) and fragile geology (as a supplier). Taiwanese rivers have been taken as a case study for rivers in Oceania where it is difficult to implement comprehensive investigation.

In this study, streamwater chemistry was monitored in two mesoscale headwater catchments for an entire year. The geographical and geological features in our study sites are distinctly different from other documented catchments to which EMMA or diagnostic tools have been applied. The concentrations of nine selected solutes, including fluoride (F), chloride (Cl), sulfate (SO₄), magnesium (Mg), potassium (K), calcium (Ca), strontium (Sr), silicon (Si), and barium (Ba), were measured. The selected catchments were monitored at a 3-day interval for a year and were supplemented by typhoon sampling at 3-h intervals. We implement the Hooper (2003) diagnostic tools because they use only the streamwater chemistry and do not require an explicit identification of end members. These tools represent one of the best choices to understand the mechanisms and the sources of solute transport in small mountainous rivers. To our knowledge, our study is the first to apply these diagnostic tools to subtropical mountainous rivers in mesoscale catchments. The objectives of this study are as follows: (1) to investigate the responses of the nine selected solute concentrations to stream discharge, (2) to apply

the diagnostic tool on streamwater chemistry to explore the number of end members, and (3) to reveal the mechanisms of catchment solute transport to small mountainous rivers. This type of investigation is useful for identifying the spatial and temporal regimes of specific biogeochemical variation and sensitivity (Salmon et al. 2001).

Study site

The Chichiawan watershed located in central Taiwan has a drainage area of 105 km² and an elevation of 1131–3882 m above sea level. In 2007–2008, the mean daily air temperature was 13.5 °C with an average of 8.9 °C in January and 17.7 °C in July. The annual runoff is approximately 3300 mm, approximately 75 % of which occurs in the wet season (May–October), primarily during the typhoon periods. The remaining months (November–April, dry season) occupy the other 25 % (Lee et al. 2013). This watershed consists of three major tributaries (Fig. 1), namely Gaoshan Creek (area=21 km²), Yikawan Creek (area=53 km²), and Yusheng Creek (area=31 km²), the three of which are the only habitat of Formosan landlocked salmon (*Oncorhynchus masou formosanus*) (Tung et al. 2006; Lee et al. 2012). In this study, the high-frequency water sampling sites were selected in Gaoshan Creek, as a model of a pristine watershed (0 % cultivated land), and in Yusheng Creek, as a model of a cultivated watershed (8.9 % cultivated land).

Two hydrological gauges monitored the water level, one for Yusheng Creek and one for the entire Chichiawan watershed (all three creeks). Consecutive water fluctuations were converted into an hourly water discharge rate using a rating curve of water discharge against water level (Herschy 1998). In 2007, the Taiwan Power Company calibrated the rating curves four times at the two gauges. Each rating curve contained a maximum of 15 measurements, ensuring reliable estimation when hourly discharges are smaller than 717 and 233 m³ s⁻¹ for Chichiawan Creek and Yusheng Creek, respectively. The discharge for Yusheng Creek was subtracted from the discharge rate at the downstream gauge (entire Chichiawan) to give the discharge for Yikawan Creek. The discharge rate for the pristine watershed was derived from the area ratio of the Gaoshan Creek watershed to the Yikawan Creek watershed (Huang et al. 2012; Lee et al. 2013). In 2007–2008, the average daily discharge rate for the Chichiawan and Yusheng creeks was 7.94 and 2.41 m³ s⁻¹, respectively. During the wet season, the average daily discharge rates for the Chichiawan and Yusheng creeks were 11.80 and 4.07 m³ s⁻¹, respectively.

The study watersheds represent the typical landscape in the mountainous regions of Taiwan, where some of the residents earn their living by growing vegetables and fruits along the riparian zone. The land use pattern is shown in Fig. 1. Natural forest, mixed forest, and secondary forest are the main land

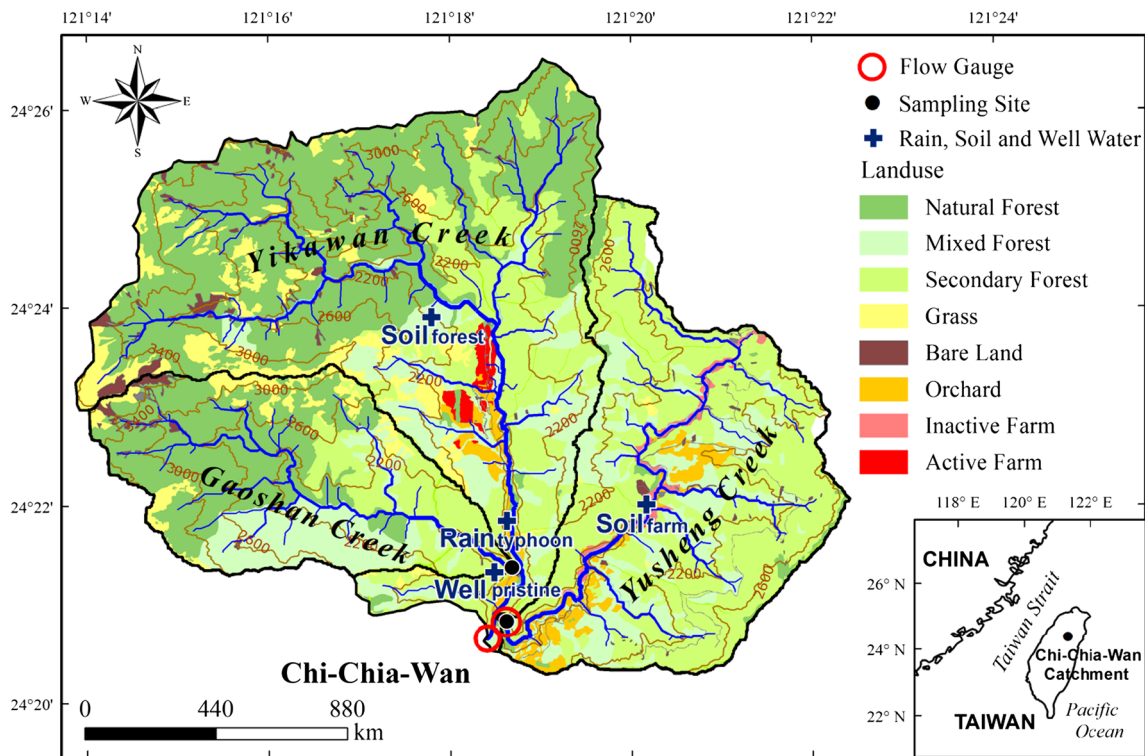


Fig. 1 Land use map of the study watershed. Streamwater samples were taken at the outlets of Gaoshan Creek and Yusheng Creek (black dots), which represent pristine and cultivated watersheds, respectively. Flow

gauge locations are given by red circles. Well samples taken from the pristine watershed and soil samples from forest and farm land are indicated by cross symbols

use types, and grass, bare land, orchard, active farm, and inactive farms are secondary land use types. To rehabilitate landlocked salmon, the cultivated farms along Yusheng Creek were expropriated by the government in 2005. The expropriated vegetable farms were categorized as inactive farms in this study. Conversely, currently operating farms, which produce mainly cabbage, are designated as active farms (Huang et al. 2012). Farmers usually apply ammonium sulfate and urea to support cabbage growth (Lee et al. 2013). Lime is always used to neutralize the acidity of the farm soil (Lin et al. 2004).

Materials and methods

Water sampling and chemistry

In non-typhoon conditions, streamwater samples from the two sites were collected twice per week and analyzed during 2007. In addition to the non-typhoon samples, two typhoons in 2007, Sepat (typhoon I, 16–19 August) and Krosa (typhoon II, 4–7 October), were sampled intensively at 3-h intervals for 72–87 h. Depth-integrated water samples were obtained using a vertically mounted 1-L bottle attached to a weighted metal frame that was gradually lowered from the bridge and applicable during typhoon period (Kao and Milliman 2008).

A well-trained local team conducted the non-typhoon sampling, and our research crews commenced the typhoon sampling shortly after the local typhoon warning system was activated. For non-typhoon sampling, water samples were immediately filtered through GF/F filters (0.7 μm) stream side and the filtrate was temporarily stored in a cooler with ice. The filtrate, approximately 15 mL, was then stored at 4 °C in a refrigerator and shipped by refrigerated container every month to the Academia Sinica for water chemistry analysis. The same procedures were conducted for typhoon samples but the filtrate was analyzed immediately after sampling. F and Cl were determined by ion chromatography (IC) using ICS-1500 instrument (Dionex, USA) with a detection limit of 0.01 mg L⁻¹. SO₄, Mg, K, Ca, Sr, Si, and Ba were determined by inductively coupled plasma–optical emission spectrometry (ICP–OES) using Optima 2100DV instrument (Perkin Elmer, USA) with a detection limit of 0.01 mg L⁻¹. For the typhoon samples, the remaining material on the filter was dried and weighed, and then the mass was divided by the volume of the filtered water sample to give the total suspended matter (TSM) in milligrams per liter.

Typhoon rain, soil, and well samples

In addition to the streamwater samples, we also considered some independently sampled end members, which should

represent the sources of the streamwater. However, it should be noted that only the typhoon rain samples taken during the study period may potentially contribute to the observed streamwater chemistry. Other end members were sampled once in April 2011 and simply used as supplementary information when discussing the changes of streamwater chemistry. Rain samples were collected during Typhoon Sepat (Rain_{typhoonI}) and Typhoon Krosa (Rain_{typhoonII}). They were collected every 3 h (in between every two streamwater samples) from the rainwater collector (Fig. 1). The collector was emptied before the next collection. Soil samples were collected as intact as possible using a sediment core of 10 cm (diameter) × 12 cm (height). Two soil samples were taken, one from an inactive farm in the cultivated watershed (Soil_{farm}) and the other from the forest of the adjacent watershed (Soil_{forest}) (Fig. 1). The soil columns were then leached with ultrapure Milli-Q water (resistivity of 18.2 MΩ-cm at 25 °C). Leaching processes were implemented for each soil column at four separate times. At each time, 50 mm in depth of Milli-Q water evenly infiltrated through the soil column and the leachate was collected below the sediment core until the soil column stopped leaching. The concentrations of dissolved solutes of each leachate were separately analyzed. Well water (Well_{pristine}) was retrieved from a well (15 m in depth) located near the outlet of the pristine watershed. Soil_{farm}, Soil_{forest}, and Well_{pristine} were snapshots, representing their chemistry at the specific sampling time. The geochemical signatures of these potential end members were analyzed, including F, Cl, SO₄, Mg, K, Ca, Sr, Si, and Ba.

Determining the number of end members

To determine the number of end members, PCA was first applied to the streamwater time series at the catchment outlet. PCA is a common technique used to explore and describe the variability of a multivariate dataset and is generally used in problems where the variation in a set of many correlated variables needs to be described by a new set of a few uncorrelated variables. This new set of variables, also called the principal components (PCs), is sorted in decreasing order of importance, that is, by the amount of variation that each component explains. The general goal of PCA is to identify a small number of PCs that can explain a substantial portion of the variation of the original variables, resulting in a lower dimensional space that explains most of the variation. The decision of how many components to retain remains subjective and is influenced by the number of input variables. The purpose of applying PCA to streamwater chemistry is to find a lower dimensional space, the U space, in which adequately describes the variability of streamwater chemistry. The dimensionality of the U space is determined by the number of eigenvectors, or PCs, that are retained from the PCA. These were determined using the “Rule of One,” where each additional eigenvector

retained should explain at least 1/(number of solutes) of variance, i.e., eigenvalue >1, in the stream chemistry (Joreskog et al. 1976). The number of PCs plus one represents the number of end members that are needed to describe the system (Christophersen and Hooper 1992; Barthold et al. 2010).

Because the maximum amount of variation in the data that can be explained is limited to that explained by the PCs retained, Hooper (2003) developed a diagnostic tool to assess the lack of fit of the data and to determine the approximate rank of the PCs. The diagnostic tool calculates the residual between the original and the projected variables. The projected variables are iteratively derived from the first PC, the first two PCs, and so on, until all the PCs are included. A random pattern of the residuals against the observed solute concentrations indicates a well-defined mixing space. Structure in the residuals indicates lack of fit in the mixing subspace, showing a non-conservative behavior of solutes or greater dimensionality (i.e., missing an end member). Curvature in the residuals can indicate chemical reactions or variable end member concentrations under some circumstances. The dimensionality of the system is then determined by the smallest dimension possible such that the residuals exhibit no structure when plotted against the observed concentrations (Hooper 2003; Barthold et al. 2010).

Bivariate solute–solute plots are usually used in advance before the application of PCA to remove those solutes that exhibit non-conservative behavior. The assumption is that streamwater chemistry is controlled by physical mixing and not by equilibrium chemistry (Christophersen and Hooper 1992; Hooper, 2003). A solute is assumed to be conservative when it exhibits at least one linear trend with one other solute. However, it is noteworthy that linear trends in solute–solute plots do not necessarily confirm conservative mixing (Hooper 2003; James and Roulet 2006). Because the non-conservative behavior of solutes can be indicated by the residual analysis, examination of bivariate solute–solute plots is not undertaken in this study to avoid the loss of information from removing solutes from the streamwater dataset.

Results

Fluctuation of discharge

The hydrographs of the two watersheds during the sampling period are illustrated in Fig. 2, showing the typical discharge pattern for Taiwan, i.e., higher discharge in the wet season (May–October) and lower discharge in other months (Kao and Milliman 2008). The dates of the two typhoon events, during which water samples were taken, are highlighted. Although these two gauges represent two neighborhood watersheds, the discharge patterns are different, indicating a shift in the baseflow. For the pristine watershed (Fig. 2a), the

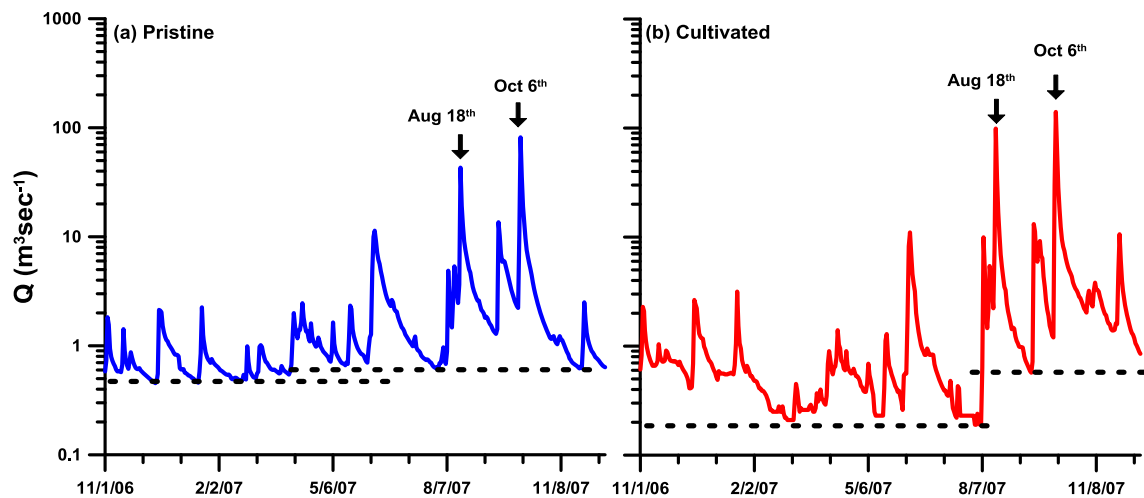


Fig. 2 Hydrograph of the **a** pristine and **b** cultivated watersheds. Arrows indicate the two typhoon events during which streamwater samples were taken

discharge varied from approximately 0.4 to 80 m³ s⁻¹ with a shift in the minimum discharge taking place around May. After May, the discharge remained higher than 0.6 m³ s⁻¹. For the cultivated watershed (Fig. 2b), the discharge was essentially similar to that of the pristine watershed in the beginning of 2007. However, the minimum discharge dropped to approximately 0.2 m³ s⁻¹ after February and remained at this level until the typhoon on August 18th. After this point, the minimum discharge increased to around 0.6 m³ s⁻¹. During the two sampled typhoons, the discharge exceeded 90 m³ s⁻¹.

Response of geochemical signatures to discharge

The relationships between geochemical concentrations and discharge (C–Q) for the nine solutes at the two watersheds are illustrated in Fig. 3. Clearly, higher concentrations were found in the streamwater of the cultivated watershed compared with those in the pristine watershed for Cl, SO₄, Mg, K, and Ca for typhoon and non-typhoon samples. F, Sr, Si, and Ba showed only subtle differences between the two watersheds, regardless of when the samples were taken. The basic statistics of the nine solute concentrations are shown in Table 1. The solute concentrations for the independently sampled end members, including the mean of Rain_{typhoon}, first leachate of Soil_{farm} and Soil_{forest}, and Well_{pristine}, are also illustrated in Fig. 3 as references. The detailed measurements of the end members are shown in Table 2 and Fig. 4.

The C–Q relationships for SO₄, Mg, Ca, and Sr concentrations showed a decrease with increasing discharge, suggesting a dilution pattern as found in other watersheds in Taiwan (Lee et al. 2009; Tsai et al. 2009; Calmels et al. 2011). The C–Q relationship of K also showed a dilution pattern but only in the cultivated watershed. Si concentrations in the typhoon samples were also diluted, while the non-typhoon concentrations were scattered at an approximately similar level. Some of the solute concentrations such as F, Cl, and Ba in both study

watersheds and K in the pristine watershed were enhanced by the discharge in the typhoon samples. During non-typhoon periods, F and Cl showed unclear C–Q relationships though relatively higher concentrations were measured at low discharges. In summary, similarities are found in the responses of any monitored solutes (except K) to the discharge in both of the study watersheds, although the magnitudes of these concentration fluctuations were different. Samples of K from the pristine watershed were slightly diluted during non-typhoon periods and enhanced during typhoon periods, in contrast to the samples from the cultivated watershed that revealed a consistent dilution pattern. Most of the measured dissolved geochemical solutes are very sensitive to discharge changes. Dilution and enhancement are related to the supply of geochemical sources and thus also to the dynamics of geochemical sources (Salmon et al. 2001).

Signatures of the sampled end members

The geochemical signatures of the sampled end members are shown in Table 2. Although these independently sampled end members do not comprehensively include all the potential end members, these sampled end members may still provide useful information about the mixing of the streamwater. The solute concentrations from the two periods of typhoon rainfall were much lower than the boundary of both the cultivated and pristine streamwater samples, with the exception of F and Cl (Fig. 4). We presume that the typhoon rainfall, collected in between our two study watersheds (Fig. 1), could be one of the potential end members for the streamwater chemistry in both of the watersheds.

For the leachate derived from the soil in the forest, F, Cl, SO₄, K, Ca, and Si concentrations clearly decreased after the first leaching process and remained at a similar level during the second to fourth leaching processes (Table 2). Other solutes’ concentrations, such as those of Mg, Sr, and Ba, do not

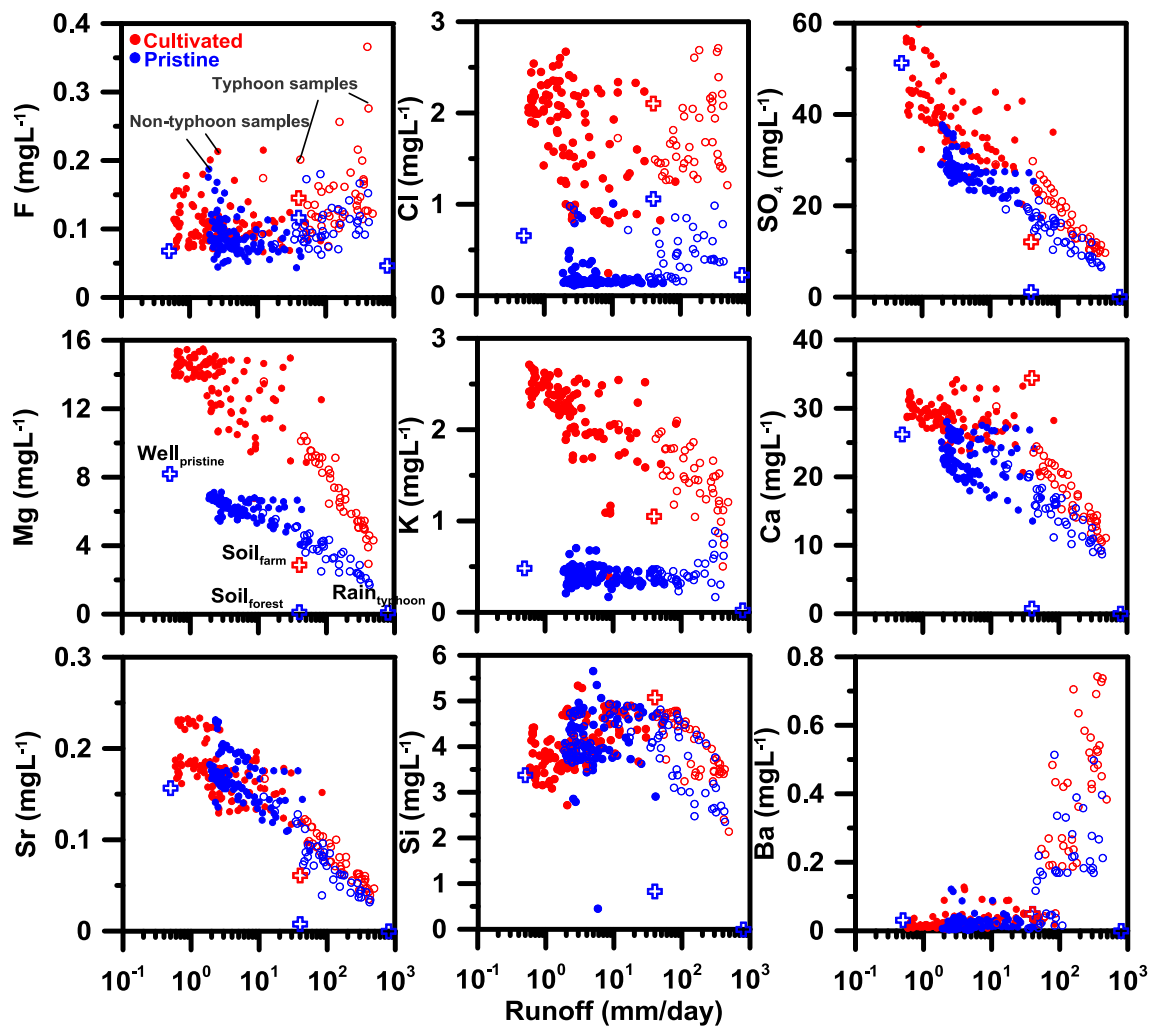


Fig. 3 Responses of streamwater chemistry to the runoff in the pristine and cultivated watersheds. Nine solutes were measured [fluoride (F), chloride (Cl), sulfate (SO_4), magnesium (Mg), potassium (K), calcium (Ca), strontium (Sr), silicon (Si), and barium (Ba)]. The pristine and cultivated data are represented by blue and red circles, respectively. Filled and empty circles stand for non-typhoon and typhoon samples,

respectively. Cross symbols represent the chemistry of the independently sampled end members, including $\text{Well}_{\text{pristine}}$, $\text{Soil}_{\text{forest}}$, $\text{Rain}_{\text{typhoon}}$ (blue crosses in the panel of Mg against runoff), and $\text{Soil}_{\text{farm}}$ (red cross). Their relative locations are similar in each panel. For the soil water, only the first leachate is illustrated. For the typhoon rainwater, the mean value of the two typhoon events is illustrated

indicate notable concentration changes, even between the first and second leachate. Because more than 90 % of the pristine and cultivated watershed areas are forested, the leachate derived in the forest soil could be one of the potential end members in both of the watersheds. The solute concentrations during the leaching processes imply that the leachate in the forest soil might represent the lower boundary of the streamwater chemistry mixing (except F, Cl, and K, see Fig. 4).

For $\text{Soil}_{\text{farm}}$, the solute concentrations are generally higher than those derived in $\text{Soil}_{\text{forest}}$ (Fig. 4). Moreover, the ranges of leachate concentration in the farm soil are wider, revealing that the leaching process clearly changes leachate concentrations. All of the solute concentrations during the leaching process show a consistent decreasing trend (although Mg and Ca concentrations increase slightly in the second leachate, see Table 2). Because $\text{Soil}_{\text{farm}}$ was taken in the cultivated

watershed, only the streamwater chemistry in the cultivated watershed is compared with the leachate chemistry of $\text{Soil}_{\text{farm}}$. The concentrations of SO_4 , Mg, K, Sr, and Ba illustrate the lower mixing boundary of the cultivated streamwater chemistry. Conversely, Ca and Si concentrations represent the upper boundary. F and Cl concentrations in $\text{Soil}_{\text{farm}}$ leachate are within the ranges of those observed in cultivated streamwater.

The well water sampled close to the outlet of the pristine watershed represented the groundwater end member in the pristine watershed. With the exception of the SO_4 and Mg concentrations in the well water, most solute concentrations were within the observed ranges of the pristine streamwater. Concentrations of Cl, K, and Ca in the well water indicated a stable source of relatively high solute concentrations. F and Si concentrations in the well water are relatively low compared with the pristine streamwater chemistry.

Table 1 Mean and standard deviation of the observed streamwater chemistry for all samples (non-typhoon and typhoon samples) in the cultivated and pristine watersheds. Nine solutes were measured

	Cultivated						Pristine					
	All data		Non-typhoon		Typhoon		All data		Non-typhoon		Typhoon	
	Ave	Std	Ave	Std	Ave	Std	Ave	Std	Ave	Std	Ave	Std
F (ppm)	0.12	0.04	0.11	0.03	0.15	0.05	0.09	0.03	0.09	0.03	0.10	0.03
Cl (ppm)	1.77	0.51	1.78	0.54	1.76	0.42	0.28	0.22	0.22	0.19	0.42	0.23
SO ₄ (ppm)	32.41	12.63	39.10	7.93	16.76	5.85	23.69	7.54	27.71	4.19	14.05	4.36
Mg (ppm)	11.51	3.45	13.38	1.77	7.13	2.22	5.49	1.40	6.25	0.58	3.66	1.08
K (ppm)	1.98	0.51	2.19	0.40	1.47	0.35	0.40	0.11	0.40	0.09	0.43	0.14
Ca (ppm)	25.23	6.20	28.67	2.44	17.17	4.63	20.49	4.87	22.81	3.08	14.92	3.72
Sr (ppm)	0.15	0.05	0.18	0.03	0.08	0.03	0.14	0.05	0.17	0.03	0.08	0.03
SiO ₄ (ppm)	4.00	0.57	4.03	0.54	3.93	0.64	4.04	0.70	4.16	0.64	3.73	0.74
Ba (ppm)	0.13	0.20	0.03	0.02	0.36	0.22	0.07	0.10	0.02	0.02	0.17	0.14

Mixing space dimensionality

We estimated the dimensionality of the streamwater chemistry recorded at each watershed using the nine solutes and applied the Rule of One, which retains eigenvectors explaining 1/9th (11 %) of the variance in streamwater solute concentrations. For the cultivated watershed, this results in two PCs, where three contributing end members account for a total of 79.5 % of the variance (Table 3). For the pristine watershed, four end members are needed to describe the system and three PCs explain a total of 79.4 % of the variance. In the cultivated watershed, the first PC is mainly explained by seven of the nine solutes, excluding Cl and Si which explain the second PC. In the first PC, SO₄, Mg, K, Ca, and Sr have positive signs; whereas, F and Ba have negative signs. In the second PC, opposite signs were derived for Cl (positive) and Si

(negative), which supports their opposite C–Q relationships (Fig. 3). In the pristine watershed, the first PC is explained by SO₄, Mg, Ca, Sr (with positive signs), and Ba (with a negative sign). F and K have a similar C–Q relationship and explain the second PC, and Cl and Si explain the third PC.

The observed solute concentrations were then projected onto the U space which is composed of new nine variables in the orthogonal coordinates (U1–U9). By the definition of orthogonality, each of these new variables will be uncorrelated with one another, and their variance is equal to the corresponding eigenvalue (Christophersen and Hooper 1992). Figure 5a illustrates the 2-D mixing space composed of U1 and U2 where the two new variables explain a total of 79.5 % of the variance in the streamwater solute concentration of the cultivated watershed. Note that the streamwater samples represented in the figure were taken under different circumstances. The

Table 2 Solute concentrations of the independently sampled end members, including rainwater from the two typhoon events (Rain_{typhoonI} and Rain_{typhoonII}), leachates of the farm (Soil_{farm}) and forest soil (Soil_{forest}), and well water from the pristine watershed (Well_{pristine})

	Soil leachate in the farm of the cultivated watershed (Soil _{farm})				Well water in the pristine watershed (Well _{pristine})	Soil leachate in the forest (Soil _{forest})				Rain (Rain _{typhoon})	
	1st leachate	2nd leachate	3rd leachate	4th leachate		1st leachate	2nd leachate	3rd leachate	4th leachate	Typhoon I	Typhoon II
F (ppm)	0.15	0.06	0.06	0.06	0.07	0.12	0.04	0.04	0.02	0.036±0.031	0.033±0.045
Cl (ppm)	2.11	0.90	0.24	0.13	0.66	1.06	0.59	0.58	0.44	0.12±0.112	0.303±0.705
SO ₄ (ppm)	12.13	5.75	2.07	1.62	51.33	1.13	0.60	0.65	0.71	0.071±0.044	0.091±0.163
Mg (ppm)	2.88	3.17	2.43	2.04	8.20	0.13	0.12	0.15	0.15	0.002±0.006	0.073±0.212
K (ppm)	1.05	0.83	0.58	0.50	0.48	0.43	0.27	0.32	0.33	0.024±0.028	0.003±0.008
Ca (ppm)	34.46	37.33	27.34	23.71	26.22	0.80	0.61	0.74	0.77	0.052±0.057	0.012±0.028
Sr (ppm)	0.06	0.06	0.05	0.04	0.16	0.01	0.01	0.01	0.01	n.a.	n.a.
Si (ppm)	5.08	4.43	3.39	3.09	3.38	0.83	0.53	0.52	0.51	n.a.	n.a.
Ba (ppm)	0.05	0.02	0.01	0.02	0.03	0.05	0.05	0.04	0.04	n.a.	n.a.

n.a. the solute concentration in the water sample is below the detection limit

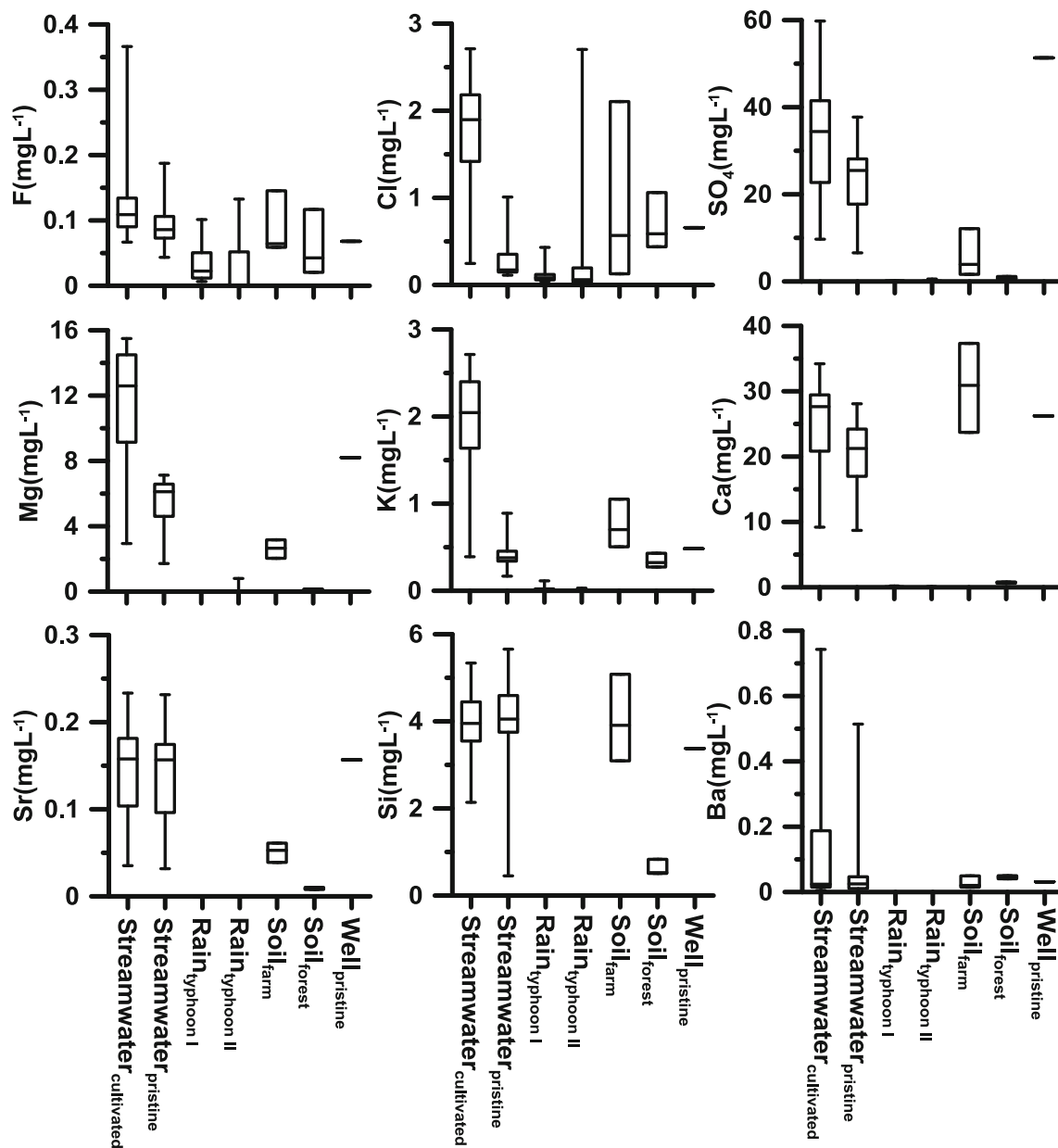


Fig. 4 Ranges of sampled water chemistry, including streamwater in the cultivated watershed ($\text{Streamwater}_{\text{cultivated}}$) and pristine watershed ($\text{Streamwater}_{\text{pristine}}$), rainwater from the two typhoon events

($\text{Rain}_{\text{typhoonI}}$ and $\text{Rain}_{\text{typhoonII}}$), leachates from the farm ($\text{Soil}_{\text{farm}}$) and forest soil ($\text{Soil}_{\text{forest}}$), and well water taken in the pristine watershed ($\text{Well}_{\text{pristine}}$)

projected values in the U space illustrate a V-shaped distribution, reflecting the temporal and hydrological variations of the samples. The shown distribution, around $U_1=0$, roughly separates the typhoon ($U_1 < 0$) and non-typhoon samples ($U_1 > 0$) (Fig. 5a). After the first typhoon, non-typhoon samples lie on pink circles while the hydrograph shifts during Aug 18th–Nov (Fig. 2b). Samples taken in December (brown circles in Fig. 5a) move toward those taken in the beginning of the year (green circles). Figure 5b shows a pattern indicating that the discharge increases with a decreasing U_1 value. To clearly reveal the discharge changes, the logarithm of discharge is shown (Fig. 5b). Green, pink, and blue/light blue circles

shown in Fig. 5a correspond to low, middle, and high discharge, respectively. An arbitrary and virtual mixing triangle could be applied onto Fig. 5a, and the vertices of the V shape could represent three unknown end members. For a streamwater observation to be explained as a convex combination of end members, it is a necessary condition that the end members exist in U space and the observations are bound in the convex sense (Christoffersen and Hooper 1992). However, residual analysis shows the residuals derived from two-dimensional mixing space, namely U_1 and U_2 , still have linear structures, which is particularly apparent for F and Si (Fig. 6). After applying the third dimension (U_3), the residuals

Table 3 Principal components and the eigenvectors derived from principal component analysis

	Cultivated			Pristine				Cultivated+pristine		
	1st	2nd	3rd	1st	2nd	3rd	4th	1st	2nd	3rd
Principal components										
Eigenvalue	5.57	1.58	0.82	4.95	1.16	1.03	0.79	4.58	2.42	0.94
Variance explained (%)	61.9	17.6	9.1	55.0	12.9	11.5	8.76	50.9	26.9	10.5
Cumulative variance explained (%)	61.9	79.5	88.6	55.0	67.9	79.4	88.2	50.9	77.8	88.3
Eigenvector										
F	<i>-0.237</i>	0.331	0.587	-0.173	<i>0.590</i>	0.294	-0.380	0.029	<i>0.537</i>	0.048
Cl	0.086	<i>0.676</i>	0.268	-0.256	0.108	<i>0.628</i>	-0.065	0.259	<i>0.662</i>	0.001
SO ₄	<i>0.388</i>	0.142	0.079	<i>0.409</i>	0.187	0.007	-0.283	<i>0.871</i>	0.002	0.016
Mg	<i>0.414</i>	0.058	0.084	<i>0.435</i>	0.095	0.139	-0.110	<i>0.883</i>	0.087	0.000
K	<i>0.378</i>	0.184	-0.050	-0.070	<i>0.716</i>	-0.234	0.614	<i>0.552</i>	0.351	0.000
Ca	<i>0.408</i>	-0.083	0.173	<i>0.407</i>	0.054	0.293	0.081	<i>0.902</i>	0.023	0.023
Sr	<i>0.398</i>	0.050	0.043	<i>0.406</i>	0.209	-0.016	-0.192	<i>0.659</i>	0.154	0.018
Si	0.049	<i>-0.560</i>	0.718	0.236	-0.189	<i>0.535</i>	<i>0.577</i>	0.046	0.129	<i>0.815</i>
Ba	<i>-0.380</i>	0.229	0.142	<i>-0.396</i>	0.001	0.271	-0.081	0.383	<i>0.474</i>	0.023

The italic numbers indicate significant variable in each PC

of Si exhibit no structure when plotted against observed Si concentration; that is, the residuals appear to be random noise. However, the residuals of F do not exhibit random noise until the application of the fourth dimension. In addition, the residuals of Ba show a linear structure, particularly for the typhoon samples. The magnitude of the residuals for Ba is reduced after adding the fifth dimension although the structure of residuals remains. In this case, four dimensions are indicated by this

analysis (Hooper 2003). This indicates that the variability of streamwater chemistry should be attributed to at least five end members, which is inconsistent with the Rule of One. Nevertheless, the residuals of Sr for the typhoon samples do not exhibit random pattern until the fifth dimension is added.

Figure 7a illustrates the 2-D mixing space for the pristine watershed. Although a V-shaped distribution is similar to the cultivated case, the projected values are relatively scattered.

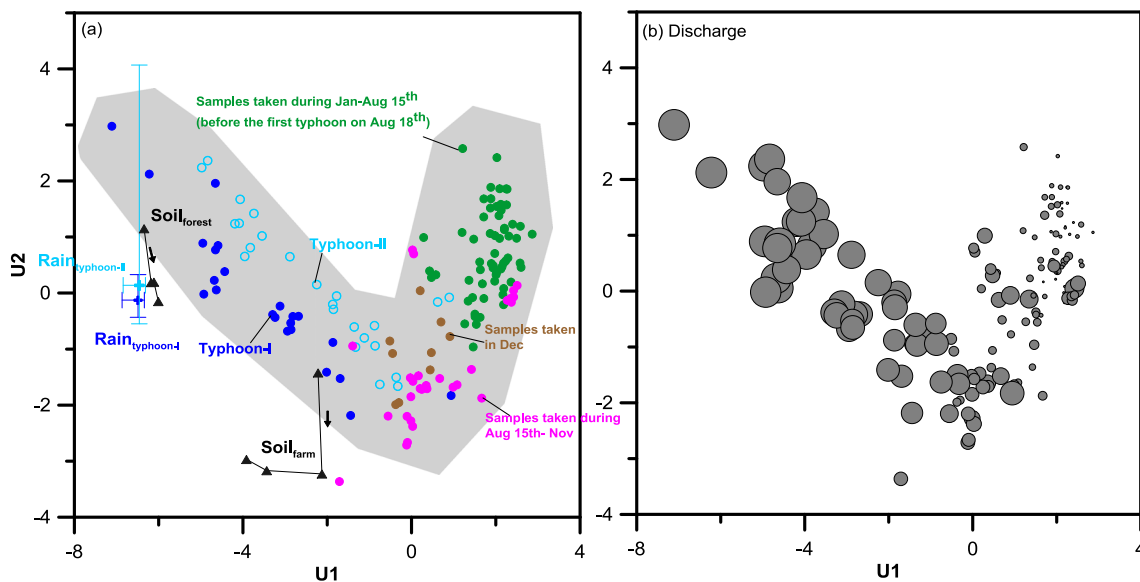


Fig. 5 a 2-D mixing space composed of the first two principal components (U1 and U2) derived from the implementation of PCA on the streamwater chemistry in the cultivated watershed. The discharge amount on the sampling day is illustrated in b where the size of the circle indicates the logarithm of the discharge. Green dots in a represent samples taken during Jan to Aug 15th. Pink and brown dots represent samples taken from Aug 15th to Nov and in Dec, respectively. Blue dots

and light blue circles represent the samples from the typhoon I and typhoon II, respectively. The independently sampled end members for the cultivated watershed are indicated by symbols as follows: Soil_{farm} (triangle), Soil_{forest} (triangle), and Rain_{typhoon} (cross). The arrow beside Soil_{forest} and Soil_{farm} samples represents the changing direction in the leaching experiment

Because use of two PCs could only explain a total of 67.9 % of the variance in the streamwater chemistry of the pristine watershed, U3 is suggested according to the Rule of One. However, three virtual end members placed around the vertices of the V-shape could essentially describe the system. Non-typhoon and typhoon samples are classified into two groups at approximately $U1 = -1$. Typhoon samples are located on the side of $U1 < -1$. The typhoon samples are more scattered in the U space than the cultivated watershed samples. Figure 7b, like Fig. 5b for the cultivated watershed, illustrates a changing discharge pattern along the U1 axis. Although the projected values are relatively scattered (Fig. 7a, compared with Fig. 5a), the locations of the projected values in the 2-D mixing space reflect the discharge amount at the sampling time. In addition to the scatter in the 2-D mixing space of the pristine watershed (Fig. 7a), non-typhoon samples are scattered along approximately $U1 = 1$, unlike the cultivated watershed (Fig. 5a) where non-typhoon samples are distributed along a diagonal line controlled by the first PC (Table 3). The results of residual analysis are shown in Fig. 8. Three dimensions, according to the Rule of One, cannot explain the variability of streamwater chemistry in the pristine watershed because the residuals of F, SO_4 , Ca, Si, and Ba do not show random patterns. At least five dimensions (six end members) are needed to describe the variability of streamwater chemistry in the pristine watershed. However, the residuals of Ca and Ba still have curvature and linear structure, even in the five-dimensional mixing space.

The independently sampled end members for the cultivated watershed, namely $Rain_{typhoon}$, $Soil_{forest}$, and $Soil_{farm}$, are also projected onto the 2-D mixing space as shown in Fig. 5a. These end members are located outside of the virtual mixing triangle. $Rain_{typhoonI}$, $Rain_{typhoonII}$, and $Soil_{forest}$ are located near the vertex when the discharge rate is high, and the $Soil_{farm}$ is located where discharge rates are intermediate. The leaching process leads $Soil_{forest}$ and $Soil_{farm}$ to move toward larger and smaller U1, respectively. We also projected $Rain_{typhoon}$, $Soil_{forest}$, and $Well_{pristine}$ onto the 2-D mixing space for the pristine watershed (Fig. 7a). The $Rain_{typhoonI}$, $Rain_{typhoonII}$, and $Soil_{forest}$ show similar locations to Fig. 5a which are near the high discharge region. Conversely, the $Well_{pristine}$ is located in the low discharge region, where groundwater dominates the hydrograph.

Discussion

Influence of hydrology and land use on streamwater signatures

Water, the carrier of the solutes from different end members, plays an important role in the identification of the potential end members. Streamwater chemistry, which simultaneously

reflects hydrological conditions, indicates different sources of water delivery to the stream (Figs. 3, 5, and 7). Streamwater chemistry is controlled by the relative input from different water masses, which each possesses distinct chemistries (e.g., Christophersen et al. 1990; Hooper et al. 1990; Evans and Davies 1998). Hydrological controls on streamwater solute concentrations usually exhibit one of the following three general C–Q relationships: dilution, enhanced hydrological access, or hydrologically constant (Salmon et al. 2001). Dilution occurs whenever the net increase in water delivery to the stream is greater than the increase in solute delivery, as shown for the cases of SO_4 , Mg, Ca, and Sr in this study (Fig. 3). The concentrations of these solutes in $Well_{pristine}$ are within the upper bounds of $Streamwater_{pristine}$ (Figs. 3 and 4). Dilution of solutes indicates a decreased relative contribution by the groundwater source. We therefore speculate that SO_4 , Mg, Ca, and Sr concentrations in the groundwater source in the cultivated watershed must be higher than $Well_{pristine}$ and $Streamwater_{cultivated}$ to result in the higher concentrations of these solutes in $Streamwater_{cultivated}$. It also implies that the influence of land use might elevate the solute concentrations in the cultivated watershed (Lee et al. 2013). Cl, SO_4 , Mg, K, and Ca are essential substances for vegetation growth. Fertilizers containing these substances accumulate in the soil and may further leach into the groundwater (Lin et al. 2004). Furthermore, the high rates of carbonate and pyrite weathering in Taiwan contribute high amounts of Ca and SO_4 to the groundwater (Goldsmith et al. 2010; Das et al. 2012). During the non-typhoon period when the rainfall intensity is low, water delivery to the stream most likely occurs through the soil. Soils on steep slopes in Taiwan are usually porous and provide an easy route for water infiltration. For the dilution cases in the pristine watershed, the solute concentrations in $Soil_{forest}$ are much lower than those in $Well_{pristine}$ (Figs. 3 and 4). When the discharge increases because the soil is saturated with water and the saturated soil boundary approaches the soil surface, the soil water delivers little solute to the stream and dilutes the streamwater. In general, the C–Q relationship shows the clearest dilution pattern when the differences in solute concentrations between deep and shallow soil water are large (Salmon et al. 2001), as indicated by $Well_{pristine}$ and $Soil_{forest}$ in this study. During typhoon periods, when the rainfall amount is large, surface runoff with depleted solute concentration further dilutes the solute concentration in the river. Surface runoff mainly originates from rainfall with lower solute concentrations (SO_4 , Mg, Ca, and Sr in Fig. 4). The abovementioned phenomena may also occur for the cultivated watershed for all solutes excluding Ca. The Ca concentration in the first leachate of $Soil_{farm}$ is higher than the range shown for $Streamwater_{cultivated}$ (Fig. 3). However, the leaching experiment shows that the Ca concentration drops significantly, further diluting the streamwater (Table 2 and Fig. 4). The significant drop might result from the rapid dissolution of calcium

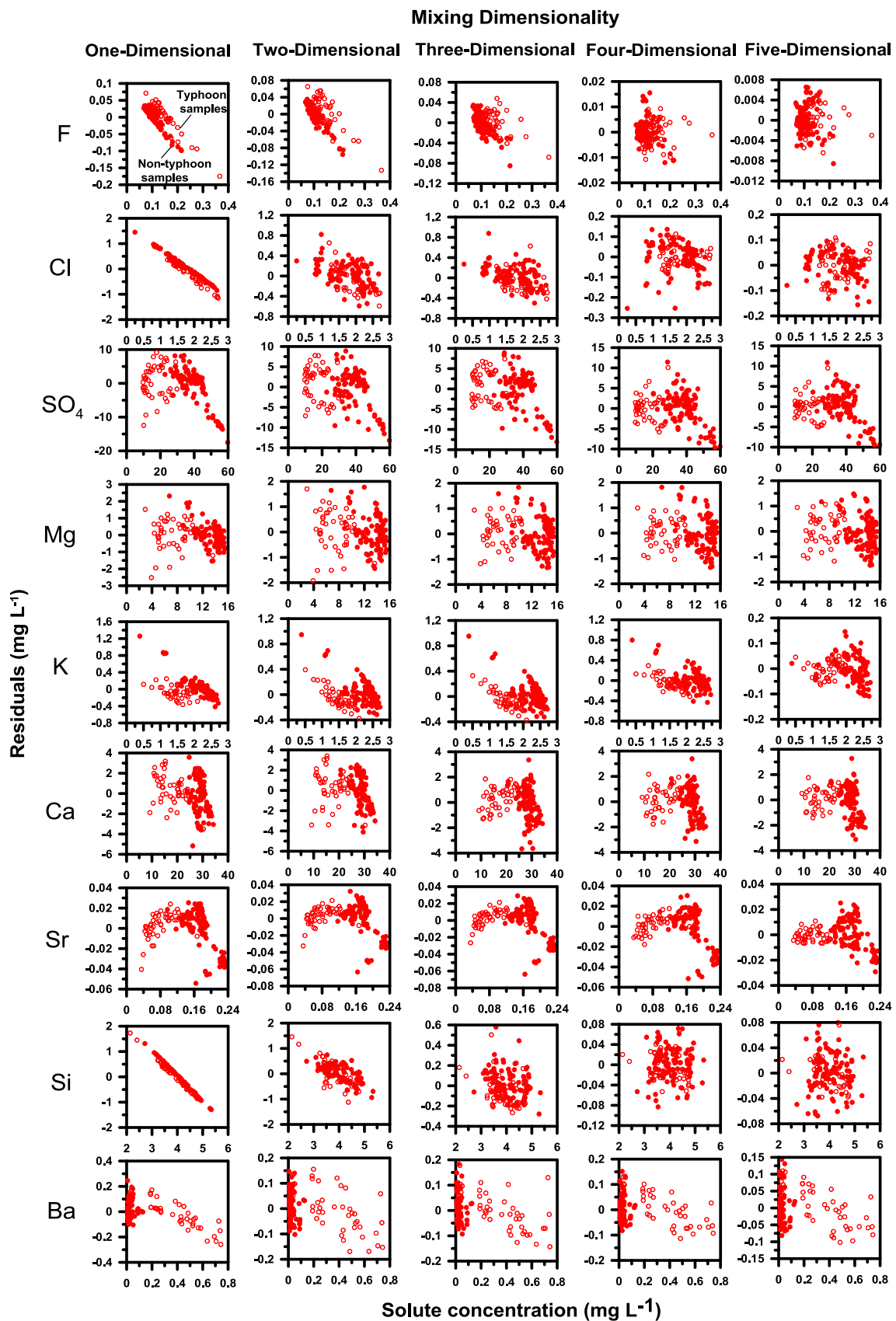


Fig. 6 Residuals fitted by increasing dimensions (principal components) and plotted against observed solute concentration in the cultivated watershed. Filled and empty circles represent non-typhoon and typhoon samples, respectively

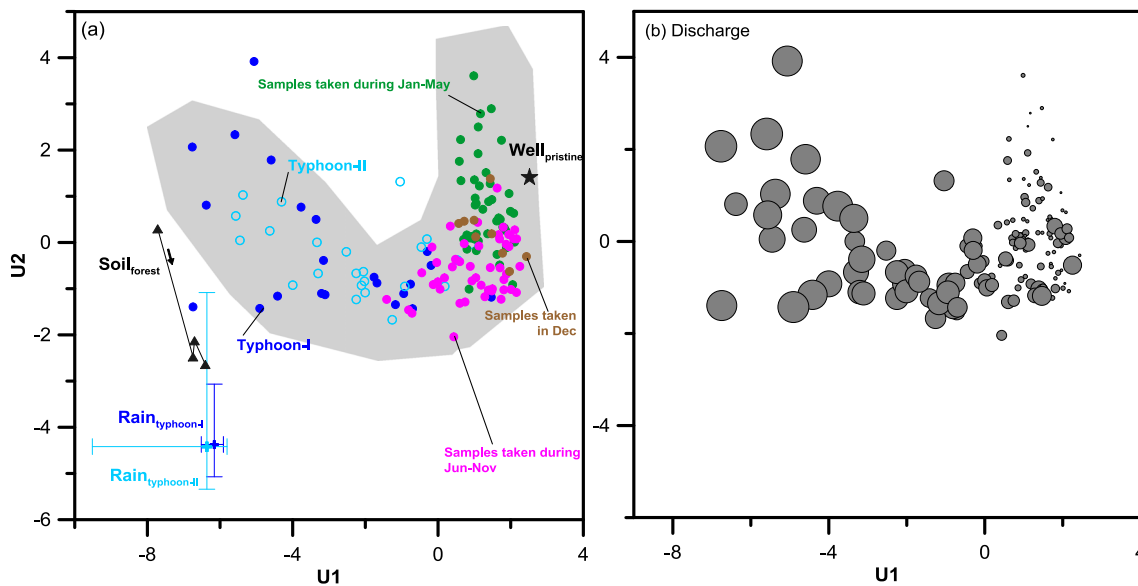


Fig. 7 **a** 2-D mixing space composed of the first two principal components (U1 and U2), derived from the implementation of PCA on the streamwater chemistry in the pristine watershed. The discharge amount on the sampling day is illustrated in **b** where the size of the circle indicates the logarithmic of the discharge. Green dots in **a** represent samples taken during Jan–May. Pink and brown dots stand for

samples taken during Jun–Nov and in Dec, respectively. Blue dots and light blue circles represent the samples from the typhoon I and typhoon II, respectively. The independently sampled end members for the pristine watershed are indicated by symbols as follows: Well_{pristine} (star), Soil_{forest} (triangle), and Rain_{typhoon} (cross). The arrow beside the Soil_{forest} represents the changing direction in the leaching experiment

carbonate (Calmels et al. 2011) as a result of lime application (Lin et al. 2004).

Enhanced hydrological access is shown by increasing solute concentration with increasing discharge, as exhibited for the cases of F, Cl, and Ba in both watersheds (and for K in the pristine watershed only); however, this only occurs in the typhoon samples (Fig. 3). There are no clear dilution or enhancement trends in the C–Q relationships of these solutes during the non-typhoon period. The most common enhanced hydrological access is shown for solutes found in areas of a watershed that are only hydrologically active during periods of high flows (Salmon et al. 2001). As the saturated soil boundary exceeds the soil surface during the typhoon period, the much lower concentrations of F, Cl, K, and Ba in the surface runoff (mainly composed of rainwater) should dilute the streamwater (Fig. 4 and Table 2). However, surface runoff that triggers soil erosion is attributable to the enhanced solute concentrations (Fig. 9). Figure 9 illustrates positive correlations between the abovementioned solute concentrations and TSM concentration during typhoon periods. We hence speculate that the concentrations of F, Cl, and Ba should be high in the surface soil particles. However, we cannot explain the inconsistent C–Q relationship of K between our two study watersheds. The associated increase in K may be linked to leaching of the vegetation and litter (Walling and Foster 1975; Miller and Drever 1977). Calmels et al. (2011) showed that the flux of K released by vegetation to the rapid surface runoff accounts for 30–56 % of the net K flux. This supports the idea that the increase of riverine K with the discharge is

related to the leaching of vegetation and litter by surface runoff (Aber and Melillo 1991), but this explanation is only valid in the pristine watershed. Lin et al. (2004) showed that potash fertilizer required by fruit growth may alter the K distribution in the soil columns in a cultivated watershed. The Si concentration of the non-typhoon samples also reveals the enhanced hydrological access, which it is particularly clear for the cultivated streamwater. The higher Si concentration in Soil_{farm} might explain the enhanced C–Q relationship (Fig. 3). However, the much lower Si concentration in the Soil_{forest} (compared to Well_{pristine}) does not result in the dilution C–Q relationship. This result requires further investigations.

Hydrologically constant control is shown by a relatively stable solute concentration, regardless of variations caused by discharge; for example, F and Ba in the non-typhoon samples of both watersheds and K in the non-typhoon samples of the pristine watershed (Fig. 3). This C–Q relationship is expected for solutes that are delivered from rainwater, which was definitely not the case in this study because the much lower concentrations of F, Ba, and K in the rainwater should dilute the streamwater (Fig. 4 and Table 2) and rainwater usually infiltrates into the soil. The most distinct dilution and enhanced hydrological access occur when the solute concentration differences between groundwater and soil water are large (Salmon et al., 2001). In other words, while the concentration differences are small, the solute concentration would remain constant as the saturated soil boundary approaches the soil surface. For the pristine watershed, the concentration differences between Well_{pristine} and Soil_{forest} are so small that the C–

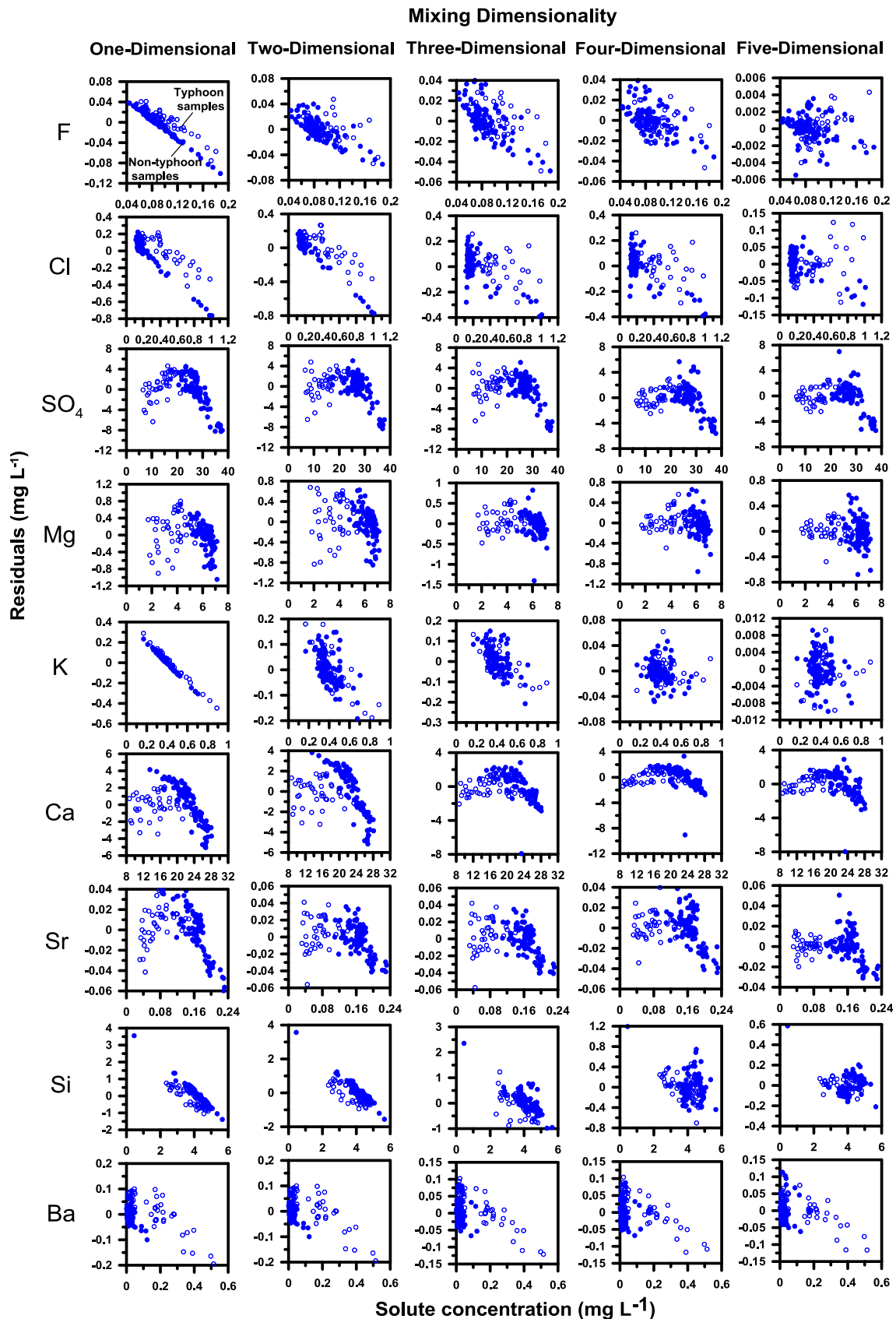
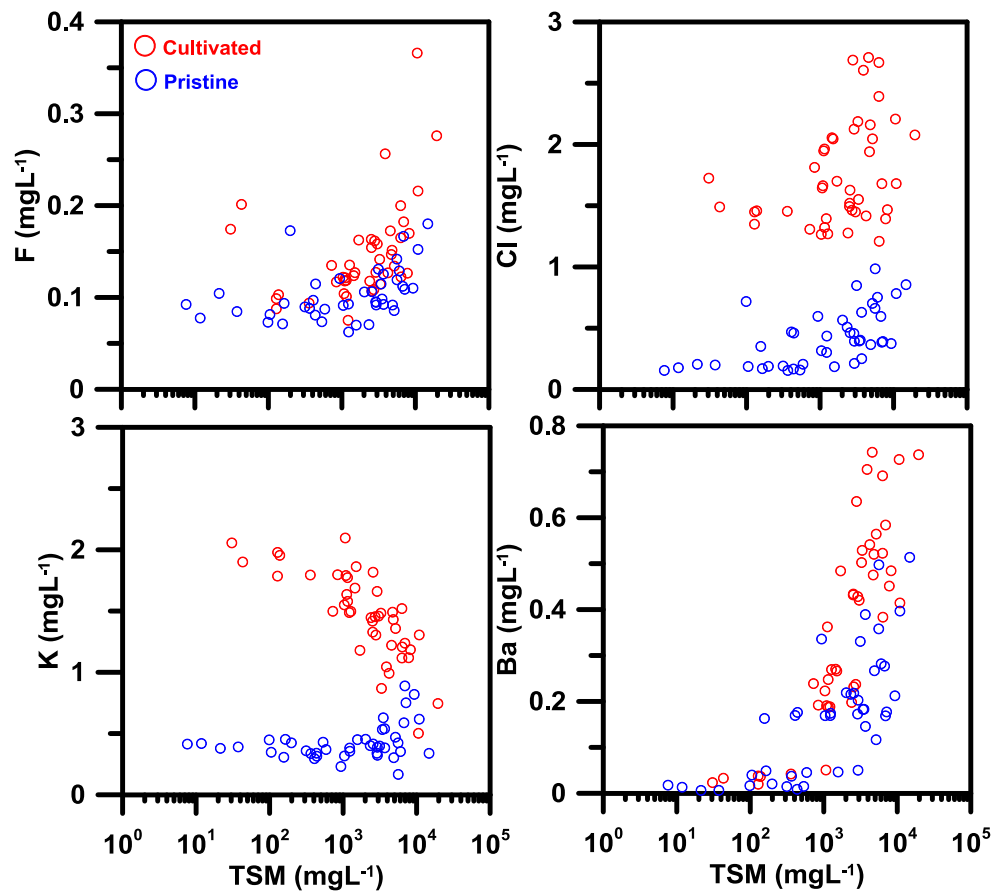


Fig. 8 Residuals fitted by increasing dimensions (principal components) and plotted against observed solute concentration in the pristine watershed. Filled and empty circles represent non-typhoon and typhoon samples, respectively

Fig. 9 Relationship between observed streamwater chemistry and total suspended matter concentration for typhoon samples in the cultivated watershed (red circles) and pristine watershed (blue circles)



Q relationships of F, K, and Ba in the non-typhoon period show hydrologically constant control. The C–Q relationship for Cl is more puzzling. Although Cl concentrations were only measured for the two typhoon events, the measurements indicate a high variation of Cl concentration in the rainwater, which might result in the observed scattered C–Q relationship (Fig. 4 and Table 2). Rainwater is the major source of Cl, particularly for watersheds located on islands (Lyons et al. 2005; Calmels et al. 2011).

Dynamic sources of solutes deliver to stream

The potential end members are projected onto the mixing space to test whether they fit well in the mixing space and bound the observed streamwater chemistry. If the end members do not lie in the U space, additional steps in the analysis are necessary to better explain the mixing system (Christophersen and Hooper 1992; Barthold et al. 2010). Figures 5a and 7a clearly illustrate all the streamwater signatures lying within a mixing triangle with three virtual end members located at the vertices of the V shape. This indicates that at least three end members circumscribe the data, which is consistent with the results derived from the Rule of One (Table 3). The vertices are closed to the projected end members, i.e., Soil_{farm} in the cultivated watershed (Fig. 5a) and

Well_{pristine} in the pristine watershed (Fig. 7a), implying the sources of the end members. In this study, the location of Well_{pristine} (close to the up-right vertex) is apparently not capable of perfectly bounding the streamwater. Groundwater is not necessarily a stable source of streamflow in terms of its geochemical signature. A previous study has demonstrated the seasonal changes of the solute concentrations of groundwater (James and Roulet 2006) which cannot be recognized by our single sample. It is very possibly true also in our case that the groundwater signature changes seasonally because some of the minimum flows are actually positioned along the line in between the upper-right and the lower-middle end members instead of being fixed at the upper-right vertex (Figs. 5b and 7b). We speculate that the lower-middle vertex is a soil water end member, although the Soil_{farm} in the cultivated mixing space (Fig. 5a) is not precisely located at the vertex. The independently sampled end members in this study did not comprehensively include all the potential end members. There are eight types of land use in our study watersheds. The Soil_{farm} samples taken in the inactive farm might not be highly representative of the soil water end members in the cultivated watershed. However, most of the water delivery to the streamflows through the inactive farms, which dominate the riparian zone (Fig. 1). Therefore, the cultivated streamwater signature is bound by the Soil_{farm} end member (Fig. 5a). In our

laboratory experiment, the $\text{Soil}_{\text{farm}}$ signature actually changes toward $\text{Rain}_{\text{typhoon}}$ with increasing leached water (Fig. 5a and Table 2). We may not provide adequate time for the water to make contact with the soil, but this still implies that the signature of the soil water end member may change if the water flowing through the farm soil is abundant and fast. However, the streamwater is still bound by the sequence of the $\text{Soil}_{\text{farm}}$ leachate, which implies a link to $\text{Soil}_{\text{forest}}$. The sequence of the $\text{Soil}_{\text{forest}}$ leachates moves toward a smaller U2. These results highlight the need to recognize the temporal variation in end member chemistry as a function of catchment wetness and the need to collect high-frequency data on streamwater as well as potential end members to better characterize catchment flow paths and mixing responses (Inamdar et al. 2013). Both $\text{Rain}_{\text{typhoon}}$ and $\text{Soil}_{\text{forest}}$ lie around the boundary of the mixing space, but not at the vertex (Fig. 5a). During the typhoon period, streamwater signatures indeed move toward $\text{Rain}_{\text{typhoon}}$ and $\text{Soil}_{\text{forest}}$. $\text{Rain}_{\text{typhoon}}$ with low solute concentrations, significantly diluting streamwater chemistry (see Fig. 3, for most of the solutes), is one of the streamwater sources. More than 90 % of watershed area is forest, leading to similar signatures of the subsurface flow and $\text{Soil}_{\text{forest}}$. For the pristine watershed without the signature of $\text{Soil}_{\text{farm}}$, the extent of leaching water of $\text{Soil}_{\text{forest}}$ bounding the edges of the typhoon samples (Fig. 7a) is much wider than those in the cultivated watershed (Fig. 5a). The area covered by $\text{Well}_{\text{pristine}}$, $\text{Soil}_{\text{forest}}$, and $\text{Rain}_{\text{typhoon}}$ could circumscribe approximately 70 % of the streamwater data. If the seasonal variability existed in the $\text{Well}_{\text{pristine}}$ end member, the streamwater chemistry could be further explained. Both Figs. 5a and 7a show an interesting pattern that has never been seen in previous studies; there is a blank region inside the mixing triangle. This indicates that every streamwater sample is mainly composed of two end members. For the non-typhoon samples, streamwater is mixed up with the upper-right and lower-middle end members. For the typhoon samples, it is mixed up with the upper-left and lower-middle end members. According to the residual analysis of Ba in Figs. 6 and 8, linear structure in the residuals of typhoon samples indicates non-conservative behavior of solutes or a missing end member (Hooper 2003). Five-dimensional mixing spaces in both watersheds still underestimate Ba concentration in the streamwater, and the magnitude of underestimation increases with increasing Ba concentration. Because the Ba concentrations of typhoon samples are positively correlated to the increasing discharge (Fig. 3), this indicates that an end member releases higher Ba concentration in higher discharges (i.e., non-conservative behavior). It might also indicate a missing end member because the structure disappears after the addition of one more dimension (i.e., six-dimensional mixing, not shown).

We believe the end member at the upper-left vertex should be relevant to the surface runoff-triggered erosion. None of the

previous relevant studies discussed the effects of soil erosion on streamwater chemistry (Elsenbeer et al. 1995; Mulholland and Hill 1997; Katsuyama et al. 2001; Joerin et al. 2002; Chaves et al. 2008). Unlike these abovementioned studies, only surface runoff (i.e., saturation excess overland flow) is considered. We emphasize that surface runoff actually influences streamwater chemistry in two forms, one is overland flow having similar chemistry to rainwater and the other is the eroded soil particle attached to particulate-associated solutes such as phosphate (Lee et al. 2013) and Ba. The Ba concentration is positively correlated to TSM concentration, indicating that the transport of Ba is highly relevant to erosion during the typhoon period (Fig. 9). The structure in the Ba residuals (Figs. 6 and 8) could be attributed to the end member of erosion. This might be one of the characteristics that the EMMA users should focus on, particularly in rapidly eroding basins such as Taiwan rivers (Kao et al. 2005). For rapidly eroding basins, such as most of the basins in Taiwan or small mountainous rivers in Oceania (Milliman and Syvitski 1992; Milliman 1995), it would be useful to distinguish the effects of the water part and the particulate-associated part of surface runoff on streamwater. For those solutes experiencing dilution during typhoon periods, three to four typhoons per year collectively account for 30–40 % of the annual solute flux (Kao et al. 2004); however, for particulate-associated solutes, typhoons could contribute as much as 80 % of the phosphate observed in our study watersheds (Lee et al. 2013). The consideration of particulate-associated solutes is also crucial for understanding the chemical weathering rate, particularly in high-sediment-yielding watersheds because of the coupling of physical and chemical weathering (Carey et al. 2002; Lyons et al. 2005; West et al. 2005).

In the mixing space of the cultivated watershed shown in Fig. 5a, we conclude that non-typhoon samples represent the mixture of groundwater (up-right vertex) and soil water (down-middle vertex) without too much signature of the surface runoff (either from rainwater or erosion at up-left vertex). Overfertilization makes the $\text{Soil}_{\text{farm}}$ a significant end member in the streamwater chemistry. Our previous study (Huang et al. 2012; Lee et al. 2013) has demonstrated that a very high nitrate yield from inactive farms, approximately $770 \text{ kg N ha}^{-1} \text{ year}^{-1}$, which is approximately 100× higher than that from forest, remains an apparent contributor to enhanced nitrate in streamwater. In other words, the solute concentrations of the water delivery to the stream would be easily altered once the water flows through the farm soil, even without too much contact time. The water traveling through farm soil is immediately labeled, even if residence time is short (Ball and Trudgill 1997). This might be explained by the fact that the streamwater solute concentrations in the cultivated watershed are higher than those in the pristine watershed, despite the agriculture-related land uses, which only occupy 8.9 % of the total watershed area (Fig. 4 and Table 1).

There is no agriculturally relevant land use in the pristine watershed. However, the streamwater signatures move toward the down-middle end member (Fig. 6a), making it very difficult to explain the mixing system partly because we did not comprehensively sample all of the potential end members in the pristine watershed. To explain the mixing system in the pristine watershed, we pooled together the streamwater data of the two study watersheds and applied PCA. PCA is used here to examine the similarity or dissimilarity of the variations within the two datasets. The U space could be also derived as shown in Fig. 10. The U1 and U2 can explain a total of 77.8 % of the variance in streamwater chemistry (Table 3). In Fig. 10, it is apparent that the cultivated and pristine streamwater data are spatially separate, suggesting that these two datasets are independent. The cultivated streamwater signatures maintain a V-shape distribution, but the pristine signatures become a straight line. The three end members (Fig. 5a) could explain the streamwater signatures in the cultivated watershed. However, it seems that only two end members are required to explain the mixing system in the pristine watershed, unlike in Fig. 7a. The total variance of the cultivated streamwater solute concentration is much larger than that of pristine streamwater solute concentrations (see Fig. 3 and 4, but values are not shown). In other words, while looking at the pristine streamwater data alone, the mixing system appears complicated because PCA requires three PCs (even more according to the residual analysis) to better explain the system (Table 3). However, the mixing system is simple within a large variance system. We speculate that in the pristine watershed, the differences in solute concentrations between groundwater and soil water end members are so indistinct that the two end members cannot be easily distinguished by PCA. Figures 5a and 7a together illustrate the ability of PCA to discriminate one data source from another. In Fig. 5a, the relative distance between $\text{Soil}_{\text{forest}}$ and $\text{Rain}_{\text{typhoon}}$ is much smaller than that of Fig. 7a. This indicates that PCA does not clearly separate these two water sources in a larger variance system (Fig. 5), given their similar solute concentrations (Fig. 4). However, PCA does completely separate these two water sources in the cultivated mixing system (Fig. 7a). This implies that in the polluted systems, some detailed streamwater sources might be masked because of the distinct solute concentration differences between the end members. Based on Fig. 10, we speculate that the cultivated data lying on $U1 > 0$ represent the influence of farm soil that cannot be found in the pristine data. The first PC is mainly controlled by SO_4 , Mg, K, and Ca (Table 3), all of which are common fertilizer components and the magnitude/variation of their concentrations in the cultivated watershed is higher than in the pristine watershed. This might be the reason that a mixing line between groundwater and soil water end member lies on approximately $U1=1$ for the pristine data (Fig. 7a) instead of on the diagonal line in Fig. 5a. The relatively uniform distribution of the solute

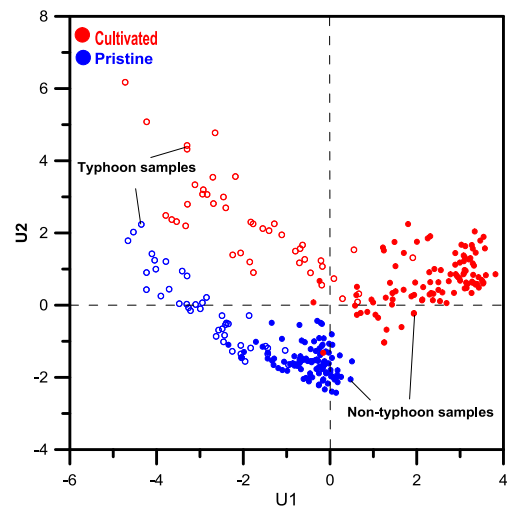


Fig. 10 First two principal components (U1 and U2) derived from the implementation of PCA on the combination of the pristine and cultivated streamwater chemistry. Red and blue circles represent streamwater samples taken in the cultivated and pristine watersheds, respectively. Filled and empty circles stand for non-typhoon and typhoon samples, respectively

concentrations in the forest soil profile might contribute to this phenomenon as well (Lin et al. 2004). Our findings align with the previous cognition that catchment systems are hydrologically complex in that they have significant flow paths below the saprolitic zone and contribute significantly to the dissolved load carried by rivers (Anderson and Dietrich 2001) and also have episodic typhoon events that wash out terrestrial material from the surface (Hilton et al. 2008; Lee et al. 2013). In this study, we did not quantitatively calculate the contribution of each end member, given the limited amount of end member samples. Moreover, Barthold et al. (2011) have also shown that the conceptual models based on EMMA are highly sensitive to the solute set size and composition, even if the moderate reproducibility of end member contributions indicates an unknown end member.

Conclusions

The detailed time series of streamwater chemistry observed in this study allows us to demonstrate the dynamics and behaviors of streamwater chemistry under changing hydrological conditions. The application of a diagnostic tool (Hooper 2003) with some independently sampled end members helps us to further identify the possible sources of the solute delivery to the stream. The two study watersheds with and without cultivation help us to understand the role of agricultural activities on affecting streamwater chemistry. According to the Rule of One, there are three and four end members for the cultivated and pristine watershed, respectively, which should explain the majority of variation of streamwater chemistry; however, the residual analysis suggests that there are at least

five and six end members, respectively. The linear structure in the residual of Ba indicates the source of erosion affecting the streamwater chemistry during the typhoon period. Our independently sampled end members somehow bound the streamwater chemistry, suggesting that groundwater, soil water, overland flow, and surface erosion are end members.

During non-typhoon periods when the rainfall intensity is low, the streamwater chemistry reveals a binary mixing between groundwater and soil water. The soil water end member in the cultivated watershed seems to be dominated by the soil water from the riparian farm. Because of fertilizer contamination of the soil, the water traveling through the farm soil in the riparian region is labeled, resulting in the vivid signature of the soil water end member in the streamwater chemistry. However, the end member samples in the pristine watershed cannot provide any evidence that one of sources in the binary mixing belongs to soil water end member during the non-typhoon period. During typhoon periods when surface runoff occurs, the majority of the streamwater chemistry can be explained by the other binary mixing, perhaps between soil water and surface runoff relevant inputs. It is found that surface runoff influences the streamwater chemistry in two ways, one is through overland flow and the other might be through the surface runoff-triggered erosion, which has never been discussed in previous studies. Two binary mixings result in a blank zone inside the mixing triangle which has also not been detected in other studies. The abundant overland flow in typhoon periods and the quick infiltration in non-typhoon periods together result in a great variability of runoff in small mountainous rivers, masking the detailed streamwater sources and impeding the application of EMMA. Previous studies also found that the short-term variation in the chemistry of the surface and shallow reservoirs, likely to be the most sensitive to rainfall intensity and/or seasonal variation in climate, will be masked by the greater variability in the relative contributions to streamflow from the major water masses (Inamdar et al. 2013). This should be a pioneering study that highlights the potential end members for the streamwater chemistry of small mountainous rivers. To comprehensively identify all the streamwater sources, time series measurement of well and soil water would be required to consider the effects of different seasons and hydrological conditions. Moreover, chemistry of surface soil particle is essential. It is particularly crucial for the regions in which there is strong discharge variability and considerable eroding ability, which are the characteristics of small mountainous rivers.

Acknowledgments We dedicate this research to Dr. Shih-Chieh Hsu, who sacrificed his life on the research cruise on October 10th, 2014. Dr. Hsu was a Research Fellow at the Research Center for Environmental Changes, Academia Sinica, Taiwan. Most of the solute concentrations in this study were analyzed by his lab. The authors also sincerely appreciate the fund support of the Ministry of Science and Technology (MOST 103-2119-M-003-006) and the field sampling support from Dr. Lin-Yan Liao

of the Shei-Pa National Park Headquarters. We also thank the Taiwan Power Company and Water Resources Agency for providing the hydrological records.

References

- Aber JD, Melillo JM (1991) *Terrestrial ecosystems*. Saunders, Philadelphia
- Acuña V, Dahm CN (2007) Impact of monsoonal rains on spatial scaling patterns in water chemistry of a semiarid river network. *J Geophysical Res: Biogeosciences* 112, G04009. doi:10.1029/2007JG000493
- Ali GA, Roy AG, Turmel MC, Courchesne F (2010) Source-to-stream connectivity assessment through end-member mixing analysis. *J Hydrol* 392:119–135
- Anderson SP, Dietrich WE (2001) Chemical weathering and runoff chemistry in a steep headwater catchment. *Hydrol Process* 15:1791–1815
- Anderson SP, Dietrich WE, Brimhall GH Jr (2002) Weathering profiles, mass-balance analysis, and rates of solute loss: linkages between weathering and erosion in a small, steep catchment. *Geol Soc Am Bull* 114:1143–1158
- Ball J, Trudgill S (1997) Potentials and limitations in using geochemical tracers. *Hydrochemistry Proc international symposium, Rabat, Morocco* 244:185–194
- Barthold FK, Wu J, Vaché KB, Schneider K, Frede HG, Breuer L (2010) Identification of geographic runoff sources in a data sparse region: hydrological process and the limitations of tracer-based approaches. *Hydrol Process* 24:2313–2327
- Barthold FK, Tyralla C, Schneider K, Vache KB, Frede H-G, Breuer L (2011) How many tracers do we need for end member mixing analysis (EMMA)? A sensitivity analysis. *Water Resour Res* 47, W08519. doi:10.1029/2011WR010604
- Burns DA, McDonnell JJ, Hooper RP, Peters NE, Freer JE, Kendall C, Beven K (2001) Quantifying contributions to storm runoff through end-member mixing analysis and hydrologic measurements at the Panola Mountain research watershed (Georgia, USA). *Hydrol Process* 15:1903–1924
- Calmels D, Galy A, Hovius N, Bickle M, West AJ, Chen M-C, Chapman H (2011) Contribution of deep groundwater to the weathering budget in a rapidly eroding mountain belt, Taiwan. *Earth Planet Sc Lett* 303:48–58. doi:10.1016/j.epsl.2010.12.032
- Carey AE, Nezat CA, Lyons WB, Kao SJ, Hicks DM, Owen JS (2002) Trace metals fluxes to the ocean: the importance of high-standing oceanic islands. *Geophys Res Lett* 29:2099
- Chang CT, Hamburg SP, Hwong JL, Lin NH, Hsueh ML, Chen MC, Lin TC (2013) Impacts of tropical cyclones on hydrochemistry of a subtropical forest. *Hydrol Earth Syst Sc* 17:3815–3826
- Chaves J, Neill C, Germer S, Neto SG, Krusche A, Elsenbeer H (2008) Land management impacts on runoff sources in small Amazon watersheds. *Hydrol Process* 22:1766–1775
- Christophersen N, Hooper RP (1992) Multivariate analysis of stream water chemical data: the use of principal components analysis for the end-member mixing problem. *Water Resour Res* 28:99–107
- Christophersen N, Neal C, Hooper RP, Vogt RD, Andersen S (1990) Modelling streamwater chemistry as a mixture of soilwater end members—a step towards second-generation acidification models. *J Hydrol* 160:307–320
- Dadson SJ et al (2003) Links between erosion, runoff variability and seismicity in the Taiwan orogen. *Nature* 426:648–651
- Das A, Chung CH, You CF (2012) Disproportionately high rates of sulfide oxidation from mountainous river basins of Taiwan orogeny: sulfur isotope evidence. *Geophys Res Lett* 39, L12404. doi:10.1029/2012GL051549

- Elsenbeer H, Lorieri D, Bonell M (1995) Mixing model approaches to estimate storm flow sources in an overland flow-dominated tropical rain forest catchment. *Water Resour Res* 31:2267–2278
- Evans C, Davies TD (1998) Causes of concentration/discharge hysteresis and its potential as a tool for analysis of episode hydrochemistry. *Water Resour Res* 34:129–137. doi:10.1029/97WR01881
- Fröhlich HL, Breuer L, Vaché KB, Frede HG (2008) Inferring the effect of catchment complexity on mesoscale hydrologic response. *Water Resour Res* 44, W09414. doi:10.1029/2007WR006207
- Goldsmith ST, Kao SJ, Carey AE, Lyons WB, Selvaraj K, Lee TY (2010) Chemical weathering in the central and coastal ranges of Taiwan. *Geochim Cosmochim Acta* 74:A343
- Herschey RW (1998) *Hydrometry: principles and practice*, 2nd edn. John Wiley & Sons, Chichester. ISBN 978-0-471-97350-8
- Hilton RG, Galy A, Hovius N, Chen MC, Horg MJ, Chen HY (2008) Tropical-cyclone-driven erosion of the terrestrial biosphere from mountains. *Nat Geosci* 1:759–762
- Hooper RP (2003) Diagnostic tools for mixing models of stream water chemistry. *Water Resour Res* 39:1055. doi:10.1029/2002wr001528
- Hooper RP, Christophersen N, Peters NE (1990) Modelling streamwater chemistry as a mixture of soilwater end-members—an application to the Panola Mountain catchment, Georgia, U.S.A. *J Hydrol* 116:321–343
- Huang JC, Lee TY, Kao SJ, Hsu SC, Lin HJ, Peng TR (2012) Land use effect and hydrological control on nitrate yield in subtropical mountainous watersheds. *Hydrol Earth Syst Sci* 16:699–714
- Inamdar S et al (2013) Temporal variation in end-member chemistry and its influence on runoff mixing patterns in a forested, Piedmont catchment. *Water Resour Res* 49:1828–1844
- James AL, Roulet NT (2006) Investigating the applicability of end-member mixing analysis (EMMA) across scale: a study of eight small, nested catchments in a temperate forested watershed. *Water Resour Res* 42, W08434
- Joerin C, Beven KJ, Iorgulescu I, Musy A (2002) Uncertainty in hydrograph separations based on geochemical mixing models. *J Hydrol* 255:90–106
- Joreskog K, Klován J, Reymont R (1976) *Geological factor analysis, methods in geomathematics*. Elsevier, Amsterdam
- Kao SJ, Milliman JD (2008) Water and sediment discharge from small mountainous rivers, Taiwan: the roles of lithology, episodic events, and human activities. *J Geol* 116:431–448
- Kao SJ, Shiah FK, Owen JS (2004) Export of dissolved inorganic nitrogen in a partially cultivated subtropical mountainous watershed in Taiwan. *Water Air Soil Poll* 156:211–228
- Kao SJ, Lee TY, Milliman JD (2005) Calculating highly fluctuated suspended sediment fluxes from mountainous rivers in Taiwan. *Terr Atmos Ocean Sci* 16:653–675
- Katsuyama M, Ohte N, Kobashi S (2001) A three-component end-member analysis of streamwater hydrochemistry in a small Japanese forested headwater catchment. *Hydrol Process* 15:249–260
- Katsuyama M, Kabeya N, Ohte N (2009) Elucidation of the relationship between geographic and time sources of stream water using a tracer approach in a headwater catchment. *Water Resour Res* 45, W06414. doi:10.1029/2008wr007458
- Lee TY, Huang JC, Carey AE, Hsu SC, Selvaraj K, Kao SJ (2009) Uncertainty in acquiring elemental fluxes from subtropical mountainous rivers. *Hydrol Earth Syst Sci Discuss* 6:7349–7383. doi:10.5194/hessd-6-7349-2009
- Lee TY et al (2012) Modeling the effects of riparian planting strategies on stream temperature: increasing suitable habitat for endangered Formosan landlocked salmon in Shei-Pa National Park, Taiwan. *Hydrol Process* 26:3635–3644
- Lee TY, Huang JC, Kao SJ, Tung CP (2013) Temporal variation of nitrate and phosphate transport in headwater catchments: the hydrological controls and land use alteration. *Biogeosciences* 10:2617–2632
- Legates DR (1995) Global and terrestrial precipitation: a comparative assessment of existing climatologies. *Int J Climatol* 15:237–258
- Li YH, Chen CT, Hung JJ (1997) Aquatic chemistry of lakes and reservoirs in Taiwan. *Terr Atmos Ocean Sci* 8:405–426
- Lin YF, Lin CY, Chou WC, Lin WT, Tsai JS, Wu CF (2004) Modelling of riparian vegetated buffer strip width and placement: a case study in Shei Pa National Park, Taiwan. *Ecol Eng* 23:327–339
- Liu C-C, Yu S-B (1990) Vertical crustal movements in eastern Taiwan and their tectonic implications. *Tectonophysics* 183:111–119. doi:10.1016/0040-1951(90)90191-A
- Lyons WB, Carey AE, Hicks DM, Nezat CA (2005) Chemical weathering in high-sediment-yielding watersheds, New Zealand. *J Geophys Res-Earth* 110, F01008. doi:10.1029/2003JF000088
- Miller WR, Drever JI (1977) Water chemistry of a stream following a storm, Absaroka Mountains, Wyoming. *Geol Soc Am Bull* 88:286–290
- Milliman JD (1995) Sediment discharge to the ocean from small mountainous rivers: the New Guinea example. *Geo-Mar Lett* 15:127–133
- Milliman JD, Farnsworth KL (2013) *River discharge to the coastal ocean: a global synthesis*. Cambridge University Press, Cambridge
- Milliman JD, Syvitski JPM (1992) Geomorphic/tectonic control of sediment discharge to the ocean: the importance of small mountainous rivers. *J Geol* 100:525–544
- Mulholland PJ, Hill WR (1997) Seasonal patterns in streamwater nutrient and dissolved organic carbon concentrations: Separating catchment flow path and in-stream effects. *Water Resour Res* 33:1297–1306
- Salmon CD, Walter MT, Hedin LO, Brown MG (2001) Hydrogeological controls on chemical export from an undisturbed old-growth Chilean forest. *J Hydrol* 253:69–80
- Tsai CJ, Lin TC, Hwong JL, Lin NH, Wang CP, Hamburg S (2009) Typhoon impacts on stream water chemistry in a plantation and an adjacent natural forest in central Taiwan. *J Hydrol* 378:290–298
- Tung CP, Lee TY, Yang YC (2006) Modelling climate-change impacts on stream temperature of Formosan landlocked salmon habitat. *Hydrol Process* 20:1629–1649
- Walling DE, Foster IDL (1975) Variations in the natural chemical concentration of river water during flood flows, and the lag effect: some further comments. *J Hydrol* 26:237–244
- West AJ, Galy A, Bickle M (2005) Tectonic and climatic controls on silicate weathering. *Earth Planet Sci Lett* 235:211–228
- You CF, Lee T, Brown L, Shen JJ, Chen JC (1988) ¹⁰Be study of rapid erosion in Taiwan. *Geochim Cosmochim Acta* 52:2687–2691